EUKARYOTIC CELL, Aug. 2007, p. 1431–1438 Vol. 6, No. 8
1535-9778/07/$08.00+0 doi:10.1128/EC.00027-07

Frataxin, a Conserved Mitochondrial Protein, in the Hydrogenosome of *Trichomonas vaginalis*▽

Pavel Dolezal,[1] Andrew Dancis,[2] Emmanuel Lesuisse,[3] Róbert Sutak,[1] Ivan Hrdý,[1] T. Martin Embley,[4] and Jan Tachezy[1]*

Department of Parasitology, Faculty of Science, Charles University in Prague, Vinicna 7, 128 44 Prague 2, Czech Republic[1]; Department of Medicine, Division of Hematology-Oncology, University of Pennsylvania, Philadelphia, Pennsylvania 19104[2]; Laboratoire d'Ingenierie des Proteines et Controle Metabolique, Departement de Biologie des Genomes, Institut Jacques Monod, Unite Mixte de Recherche 7592 CNRS-Universites Paris 6/7, 2 Place Jussieu, F-75251 Paris cedex 05, France[3]; and Division of Biology, The Devonshire Building, Newcastle University, Newcastle upon Tyne, NE1 7RU, UK[4]

Received 23 January 2007/Accepted 5 June 2007

Recent data suggest that frataxin plays a key role in eukaryote cellular iron metabolism, particularly in mitochondrial heme and iron-sulfur (FeS) cluster biosynthesis. We have now identified a frataxin homologue (*T. vaginalis* frataxin) from the human parasite *Trichomonas vaginalis*. Instead of mitochondria, this unicellular eukaryote possesses hydrogenosomes, peculiar organelles that produce hydrogen but nevertheless share common ancestry with mitochondria. *T. vaginalis* frataxin contains conserved residues implicated in iron binding, and in silico, it is predicted to form a typical α-β sandwich motif. The short N-terminal extension of *T. vaginalis* frataxin resembles presequences that target proteins to hydrogenosomes, a prediction confirmed by the results of overexpression of *T. vaginalis* frataxin in *T. vaginalis*. When expressed in the mitochondria of a frataxin-deficient *Saccharomyces cerevisiae* strain, *T. vaginalis* frataxin partially restored defects in heme and FeS cluster biosynthesis. Although components of heme synthesis or heme-containing proteins have not been found in *T. vaginalis* to date, *T. vaginalis* frataxin was also shown to interact with *S. cerevisiae* ferrochelatase by using a Biacore assay. The discovery of conserved iron-metabolizing pathways in mitochondria and hydrogenosomes provides additional evidence not only of their common evolutionary history, but also of the fundamental importance of this pathway for eukaryotes.

In eukaryotes, mitochondrial proteins play vital roles in cellular iron metabolism by inserting iron into two types of prosthetic groups: FeS clusters and heme. While the steps mediating porphyrin synthesis are partitioned between mitochondria and the cytosol, the final insertion of ferrous iron into the porphyrin ring occurs in the mitochondria by the activity of ferrochelatase (7). FeS cluster biosynthesis is catalyzed by a multiprotein machinery (25, 37) with a predominantly mitochondrial localization, although in higher eukaryotes, subpopulations of some components with extramitochondrial localizations were identified (31). The process is initiated by sulfur release from free cysteine by the activity of the cysteine desulfurase IscS (47). A protein-bound persulfide is combined with a still-undefined iron intermediate to form an FeS cluster on the scaffold protein IscU. Both the heme and FeS cluster synthesis pathways rely on an iron donor within the mitochondria to distribute iron, maintain its bioavailability, and reduce its deleterious effects via Fenton chemistry. The nature of such an iron donor remains unclear; however, the small mitochondrial protein frataxin is currently the leading candidate for this function.

In humans, loss of frataxin function leads to the neurodegenerative disorder Friedreich's ataxia, which is manifested on the cellular level by mitochondrial iron accumulation, sensitivity to oxidants, depletion of mitochondrial DNA, impaired respiration, and decreased activities of FeS proteins (6, 13, 23, 45). Because of the difficulties in distinguishing between primary and secondary frataxin-associated phenotypes, the actual biochemical function of frataxin remains unresolved. However, the characterization of the yeast *Saccharomyces cerevisiae*'s frataxin homologue (Yfh1) suggests several iron-related functions. (i) In vitro studies suggest that frataxin forms large complexes with iron, which may be a mechanism for iron detoxification, reminiscent of the function of the iron storage protein ferritin (14). (ii) The participation of frataxin in FeS cluster assembly was demonstrated by its iron-dependent association with IscU or the IscS/IscU complex (15), where frataxin delivers iron to IscU (46). (iii) Recently, frataxin was shown to protect the FeS cluster of mitochondrial aconitase, functioning as an iron chaperone in the conversion of the inactive [3Fe-4S] form into the active [4Fe-4S] form of the enzyme. (iv) Based upon the observation of reduced cytochrome levels in a Δ*yfh1* strain, frataxin was also suggested to participate in heme synthesis (23). In these studies, zinc protoporphyrin was found in the affected cells instead of heme, indicating a lack of iron for the insertion step. Frataxin was further shown to physically interact with ferrochelatase in vitro, suggesting its involvement in ferrochelatase-mediated iron chemistry.

To date nothing is known about the presence and possible functions of frataxin in eukaryotes, such as *Trichomonas*, *Giardia*, and *Entamoeba*, that lack typical mitochondria. These

* Corresponding author. Mailing address: Department of Parasitology, Charles University, Faculty of Science, Vinicna 7, 128 44 Prague, Czech Republic. Phone: (420) 221951813. Fax: (420) 224919704. E-mail: tachezy@natur.cuni.cz.

▽ Published ahead of print on 15 June 2007.

unicellular organisms inhabit oxygen-poor environments, and their energy metabolism relies upon the glycolytic breakdown of glucose within the cytosol. While in *Giardia* and *Entamoeba*, pyruvate is further oxidized by cytosolic pathways, in *Trichomonas vaginalis*, pyruvate breakdown takes place in double membrane-bound organelles called hydrogenosomes. The key hydrogenosomal enzymes (PFO and hydrogenase), as well as the components of the hydrogenosomal electron transport chain (ferredoxin and the NADH dehydrogenase complex), are FeS proteins. The FeS clusters of these proteins are assembled within hydrogenosomes by a mitochondrion-type machinery involving a hydrogenosomal homologue of IscS (38, 39). In this paper, we describe a homologue of frataxin in *T. vaginalis*. Based upon its hydrogenosomal localization, its biochemistry, and its ability to complement the function of a yeast mitochondrial mutant, we conclude that frataxin in hydrogenosomes is functionally orthologous to the mitochondrial protein implicated in cellular iron metabolism.

MATERIALS AND METHODS

Cultivation and cell fractionation. *T. vaginalis* strain T1 was maintained in Trypticase-yeast extract-maltose medium with 10% heat-inactivated horse serum at 37°C. Cytosolic and hydrogenosomal fractions were prepared as described in reference 38.

Cloning and sequence analysis. A sequence encoding a nearly complete frataxin homologue was identified in a *T. vaginalis* G3 expressed sequence tag library and used to isolate a full-length sequence from a *T. vaginalis* T1 λ ZAPII genomic library (39). The probe for library screening was generated by PCR using the specific primers 5′-GTATAATGGGATATGGAG-3′ and 5′-CTTCT GTTAAACAAAC-3′. The PCR products were labeled using a random primer DNA labeling system (Invitrogen). Positive clones were sequenced and compared with bacterial and mitochondrial frataxin protein sequences in GenBank. The sequences were aligned using ClustalX (40), and the alignment was refined manually.

RNA transcription. The synthesis of nascent mRNA was assessed in lysolecithin-permeabilized cells (43). The following primer pairs were used in PCR amplifications: frataxin, 5′-ATGTTAAGCGGATTT-3′ and 5′-TTAGCAACCG AAAGC-3′; β-tubulin, 5-CATCGTCCCATCTCCAAAGG-3 and 5-AATGGA ACAAGGTTGACAGC-3; hydrogenosomal malic enzyme, 5-AGGAAGAACG TGACCGCC-3 and 5-GTTGCCGATATCGTGGTC-3; PFOR, 5′-GAYGGHA CHGTNGGHGC-3′ and 5′-TCRWADGCCCARCCRTC-3′; and Tvh-47, 5′-A TGCTTGCAGCATAC-3′ and 5′-TTACTCAGCGACGCA-3′.

Selectable transformation of *T. vaginalis*. The complete frataxin open reading frame was inserted into TagVag (19) by the use of the following specific PCR primers containing NdeI/BamHI restriction sites: 5′-CATATGTTAAGCGGAT TT-3′ and 5′-GGATCCGCAACCGAAAGC-3′. The trichomonad cells were electroporated with the plasmid and selected as described in reference 38.

Immunofluorescence microscopy. The hemagglutinin (HA)-tagged versions of *T. vaginalis* frataxin and hydrogenosomal malic enzyme were visualized in fixed *T. vaginalis* cells by using mouse anti-HA monoclonal antibody (MAb) and rabbit anti-malic enzyme polyclonal antibody as described in reference 38.

Biacore experiments. The recombinant yeast ferrochelatase was overproduced in *Escherichia coli* and purified as previously described (7, 16). The open reading frame coding for the mature frataxin lacking the putative hydrogenosomal-targeting sequence was cloned into pET28a (Novagen). The six-His-tagged recombinant protein was expressed in *E. coli* strain BL21(pLys) and purified on Ni(II)-nitrilotriacetic resin according to the manufacturer's protocol (QIAGEN). For antibody preparation, the protein was purified under denaturing conditions. For the Biacore assay, the soluble protein was diluted with the running buffer (150 mM NaCl, 0.005% Tween 20, 20 mM HEPES, pH 7.5) and incubated for one hour at 4°C with nickel resin. The resin with bound protein was transferred onto a 5-ml chromatographic column and washed with 20 ml of running buffer supplemented with 10 mM imidazole. The protein was eluted with 3 ml of running buffer with 400 mM imidazole. The eluate was loaded on a Sephacryl 300 HR (Pharmacia) column equilibrated with the running buffer. Frataxin-containing fractions were pooled and concentrated using a Centriplus concentrator (Amicon) with a 10-kDa cutoff (Millipore). The purity of the final preparation was checked by sodium dodecyl sulfate-polyacrylamide gel electrophoresis on a Coomassie-stained 14% gel.

The direct interaction between ferrochelatase and *T. vaginalis* frataxin was monitored by using a real-time biomolecular interaction analyzer, Biacore 2000, based on plasmon surface resonance measurements. *T. vaginalis* frataxin (200 resonance units [RU]) was immobilized on research grade CM5 sensor chips (Biacore) using a standard amine-coupling procedure. Control experiments were run using bovine serum albumin (200 RU) and blank flow cells (activated carboxyl groups reacted with excess ethanolamine). The circulating ferrochelatase was at a concentration of 1×10^{-7} M.

Complementation assay. The complete open reading frame of the *T. vaginalis* frataxin gene was amplified and cloned into the pEMBlyex4i vector using the NdeI and XhoI sites. The mature version of the *T. vaginalis* frataxin gene was cloned in frame behind the CoxIV mitochondrial-targeting presequence within the pEMBlyex4i vector using the XbaI and XhoI restriction sites. The vectors were linearized with StuI in the URA3 gene and used for transformation of an *S. cerevisiae* Yfh1 shuffle strain (17). The transformants were selected for uracil prototrophy, and after removal of the covering plasmid containing YFH1, LEU2, and CYH2 by counterselection on YPAD (yeast extract-peptone-dextrose plus adenine) with 10 μg/ml cycloheximide, transformants were tested for growth under inducing conditions (1% yeast extract, 2% peptone, 0.01% adenine, 2% raffinose, and 0.5% galactose) for the GAL10 promoter of the integrated pEMBlyex4i vector.

Other methods. Aconitase and malate dehydrogenase activities were measured spectrophotometrically in mitochondrial extracts (5, 28, 34). The low-temperature (−191°C) spectra of whole cells were recorded as described previously (30).

RESULTS

Analysis of the *T. vaginalis* frataxin gene. The complete sequence of the frataxin gene from *T. vaginalis* was obtained from a *T. vaginalis* genomic DNA library clone. The isolated clone contained a single putative open reading frame without intron-like sequences and coded for a protein of 121 amino acids in length. The predicted molecular mass and isoelectric point for the putative *T. vaginalis* frataxin were 13.8 kDa and 4.9, respectively. Similar acidic pI values have been reported for all frataxin homologues, reflecting the high content of Asp and Glu residues in the protein.

BLASTP searches yielded the highest scores with eukaryotic and eubacterial (CyaY) frataxin homologues. No frataxin homologue has been identified in any archaebacterial species so far. The protein sequence of *T. vaginalis* frataxin was compared with those of its homologues from eubacteria and eukaryotes (Fig. 1). In eukaryotes, the sequence of the mature protein is typically preceded by a variable N-terminal region that carries a mitochondrial-targeting signal sequence. The structures of human, yeast, and bacterial frataxin have been solved recently (10, 12, 18), showing that these homologues are defined by an α-β sandwich motif, with two N-terminal and C-terminal α-helices forming a helical plane above five antiparallel β-strands forming a β-sheet plane. While the β-sheet plane is rather neutral in charge, the helical plane and the H1-S1 interface contain conserved and exposed acidic residues (18). Possible iron-binding residues were identified in this region and are conserved in the *T. vaginalis* homologue (Fig. 1), suggesting that it may have similar iron-binding properties. Using the SWISS-MODEL program (http://swissmodel.expasy.org//SWISS-MODEL.html) (35), the theoretical structure of *T. vaginalis* frataxin was derived, using human frataxin as a template. The model of *T. vaginalis* frataxin revealed that the predicted polypeptide chain could form the characteristic frataxin α-β sandwich motif (Fig. 2). No structure was assigned to three loops of the polypeptide chain due to the lack of sequence similarity between homologues in these regions.

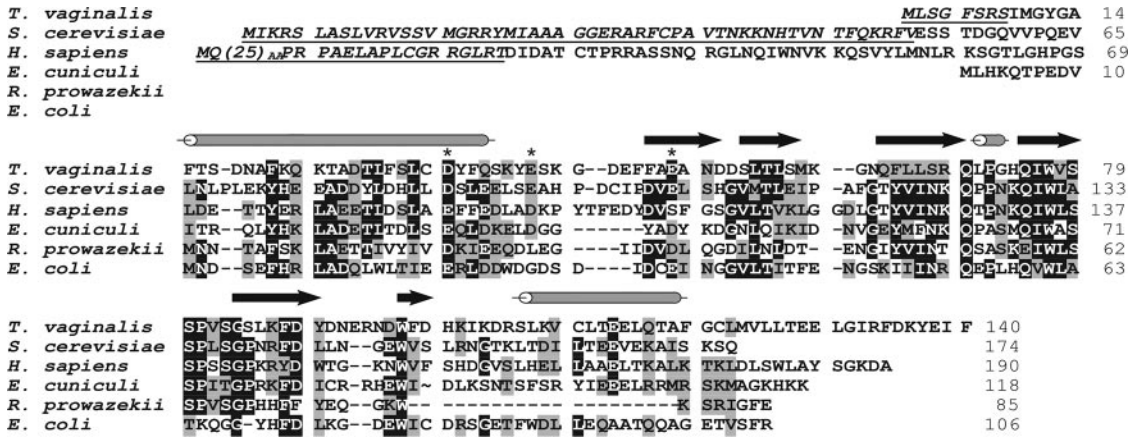

FIG. 1. Multiple protein sequence alignment of eukaryotic and eubacterial frataxin homologues. The proteins were aligned using the ClustalX program (40). The black shading indicates where identical amino acids are conserved; the gray shading shows similar amino acids, with the threshold set to 50%. The mitochondrial-targeting and putative hydrogenosomal sequences are in italics and underlined. In the human frataxin sequence, 25 N-terminal amino acids were omitted from the alignment. Asterisks denote identical/similar residues implicated in iron binding, which are conserved in *T. vaginalis* frataxin. Secondary-structure elements of *E. coli* CyaY are indicated above the sequence alignment (according to reference 10).

Transcription of the *T. vaginalis* frataxin gene. The analysis of the 5′ upstream region preceding the *T. vaginalis* frataxin gene open reading frame did not reveal the presence of a conserved initiator (Inr) element (Fig. 3A). This element, consisting of $TCA_{+1}YT/A$ as a consensus sequence, determines the transcription start site (at A_{+1} position) and has been found in all *T. vaginalis* genes examined so far (26). The mRNAs of *T. vaginalis* possess unusual short 5′ untranscribed regions of about 10 to 17 bp before the translation start, and the modification of the Inr consensus sequence results in the generation of mRNAs with inaccurate transcription start sites, thereby interfering with gene expression (26). The transcription of the frataxin gene was therefore verified by monitoring mRNA synthesis in permeabilized cells (Fig. 3B).

In *S. cerevisiae*, frataxin expression is stimulated by iron (32, 33), and iron has also been shown to dramatically regulate the metabolism of trichomonads (42). During iron deficiency, the expression of key hydrogenosomal enzymes (e.g., PFO and hydrogenase) dramatically decreases and overall glucose metabolism is shifted towards cytosolic glycolytic breakdown. The synthesis of mRNA under iron-rich and iron-restricted conditions was monitored to examine the possible effects of iron availability on the transcription of the *T. vaginalis* frataxin gene. Whereas the transcription of *pfo* and *tvh-47* was decreased under iron-restricted conditions, *T. vaginalis* frataxin gene transcription increased about threefold (Fig. 3B), in contrast to the data obtained from yeast and human cells.

Cellular localization of *T. vaginalis* frataxin. In eukaryotes, frataxin is localized primarily in the mitochondria, although a small amount of extramitochondrial frataxin has recently been

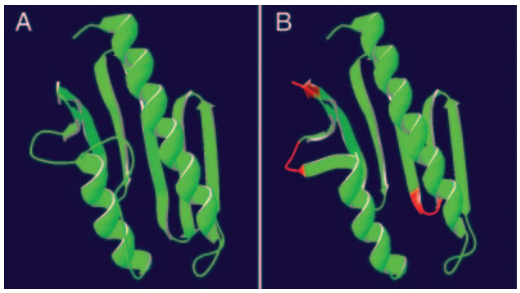

FIG. 2. Model of *T. vaginalis* frataxin. The three-dimensional structure of *T. vaginalis* frataxin was deduced by using the theoretically translated frataxin sequence (B). The previously solved crystal structure of human frataxin (PDB accession number 1EKG) was used as a template (A). The primary sequence alignment was generated by using ClustalW (http://www.ebi.ac.uk/clustalw), edited manually and submitted to SWISS-MODEL (http://swissmodel.expasy.org//SWISS-MODEL.html) (35). The unmodeled regions of *T. vaginalis* frataxin are shown in red.

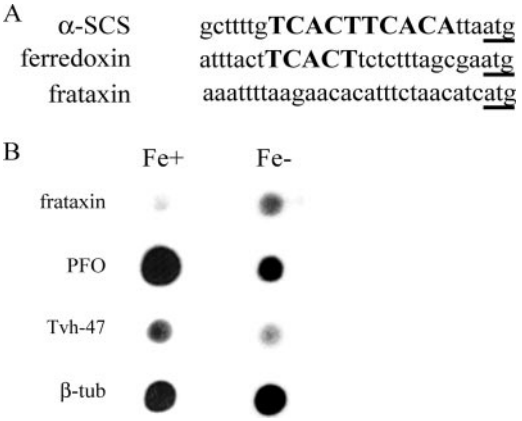

FIG. 3. Transcription of *T. vaginalis* frataxin gene. (A) Conserved motifs of putative initiator elements (in uppercase) in the sequences of 5′ regions preceding the open reading frame of the *T. vaginalis* α subunit of succinyl-coenzyme A synthase (α-SCS), ferredoxin, and frataxin. The nucleotides corresponding to the start codons are underlined. (B) Synthesis of nascent RNA. Cells maintained under iron-rich (Fe^+) or iron-restricted (Fe^-) conditions were permeabilized with lysolecithin and incubated with buffer containing [^{32}P]UTP. Total RNA was isolated and hybridized to specific DNA probes. PFO, pyruvate:ferredoxin oxidoreductase; Tvh-47, subunit of hydrogenosomal NADH dehydrogenase complex; β-tub, β-tubulin.

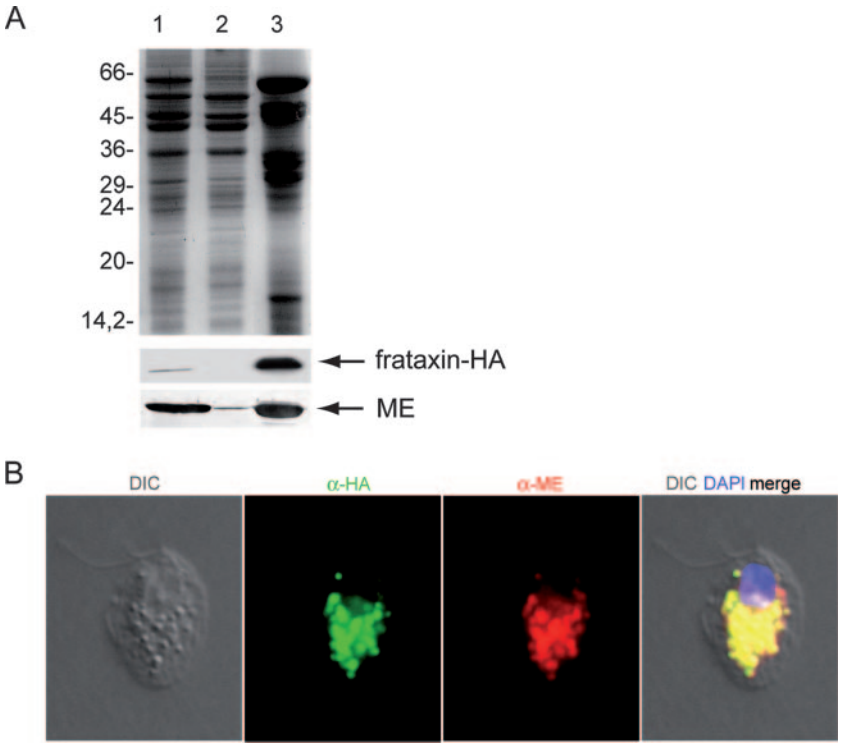

FIG. 4. Cellular localization of *T. vaginalis* frataxin. (A) The cellular fractions of *T. vaginalis* overexpressing HA-tagged frataxin were analyzed by sodium dodecyl sulfate-polyacrylamide gel electrophoresis (top) and Western blotting (bottom). The tagged frataxin and hydrogenosomal malic enzyme, a marker for hydrogenosomes, were detected by mouse anti-HA MAb and by anti-malic enzyme polyclonal antibody, respectively. 1, total cell lysate; 2, cytosol; 3, hydrogenosomes; ME, malic enzyme. Molecular mass markers in kDa are shown on the left. (B) Immunolocalization of frataxin in hydrogenosomes of *T. vaginalis*. The tagged frataxin was detected by mouse anti-HA MAb and Alexa Fluor 488 (green) donkey anti-mouse immunoglobulin G. Malic enzyme was detected by anti-malic enzyme polyclonal antibody, Alexa Fluor 546 (red) donkey anti-rabbit immunoglobulin G. The nuclei were stained with 4′,6′-diamidino-2-phenylindole (DAPI). DIC, differential interference contrast; α, anti.

described in human cell lines (11). Efficient delivery into the organelle is ensured by the presence of an N-terminal targeting sequence that is cleaved upon protein translocation. As previously shown (39), the prediction software designed to identify mitochondrial-targeting signals can sometimes be successfully used for the detection of signals on hydrogenosomal proteins. PSORT II (http://psort.ims.u-tokyo.ac.jp) was used to predict the localization of *T. vaginalis* frataxin. A mitochondrial/hydrogenosomal localization was predicted with 45% confidence and was further supported by the identification of a putative cleavage site for the organellar processing peptidase (SRS/IM) with a characteristic arginine at position −2 relative to the cleavage site. We overexpressed *T. vaginalis* frataxin with a C-terminal HA tag in trichomonads, and Western blot analysis of the cellular fractions showed the presence of recombinant *T. vaginalis* frataxin in the cell homogenate and purified hydrogenosomes (Fig. 4A). The estimated molecular mass of about 16 kDa corresponded to the theoretical frataxin size, including the double HA tag.

By means of immunofluorescence microscopy, the HA-tagged version of *T. vaginalis* frataxin was localized within numerous organelles surrounding the nucleus and main cytoskeletal structures (Fig. 4B). These organelles correspond to hydrogenosomes, as demonstrated by the colocalization of the HA tag signal with hydrogenosomal malic enzyme in a double-labeling experiment.

Complementation of yeast frataxin mutants. Previous studies reported the defective respiration, unstable mitochondrial DNA, and hypersensitivity to oxidative stress that follow inactivation of the yeast frataxin homologue (Yfh1) (6, 20). The impairment of mitochondrial iron metabolism, particularly FeS cluster and heme synthesis, was suggested to be the primary cause for this complex phenotype (48). To study the function of *T. vaginalis* frataxin, we tested its ability to complement the Yfh1 function in yeast.

One of the difficulties when working with Δ*yfh1* cells is that suppressor mutations occur with high frequency (23). For this reason, we used a Yfh1 shuffle strain (17), in which a covering plasmid bearing the wild copy of *YFH1* can be ejected by growing the cells with cycloheximide. The complete *T. vaginalis* frataxin and chimeric CoxIV-*T. vaginalis* frataxin product, comprising the CoxIV mitochondrial-targeting sequence and the *T. vaginalis* frataxin sequence minus its hydrogenosomal-targeting sequence, were each used to transform the Yfh1 shuffle strain. The wild-type *YFH1* open reading frame and no open reading frame were used as the positive and negative controls, respectively. The expression of all constructs was under the control of the Gal promoter. The transformants were plated onto yeast extract-peptone-dextrose agar plates and then transferred to cycloheximide-containing YPAGal (yeast extract-peptone-adenine-galactose) plates to eject the covering plasmid. Significant growth differences were observed (Fig. 5).

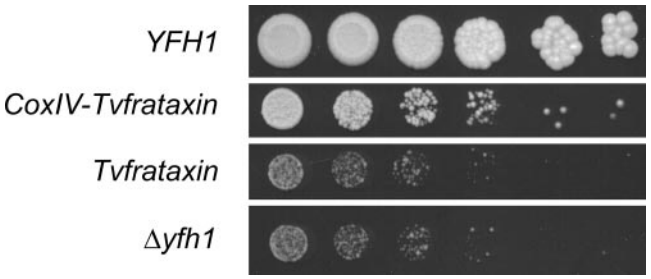

FIG. 5. Complementation of a yeast mutant deficient in frataxin (Δyfh1). The gene for *T. vaginalis* frataxin (Tvfrataxin) and a chimeric construct containing genes for the mitochondrial-targeting sequence of CoxIV and for *T. vaginalis* frataxin (CoxIV-Tvfrataxin) truncated at the N terminus to remove the putative hydrogenosomal-targeting signal were integrated into the genome of the Δ*yfh1* mutant under the control of the Gal1 promoter mutant by using the shuffle strategy. Wild-type *YFH1* and the empty vector (Δ*yfh1*) served as the positive and negative controls, respectively. Serial 10-fold dilutions of 10^6 cells are shown.

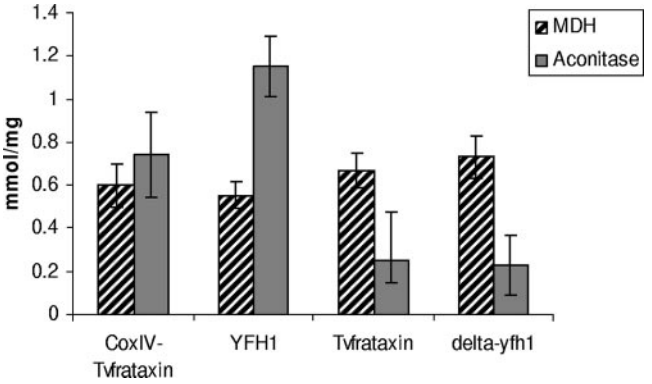

FIG. 6. Aconitase activity in the complemented yeast strain. The levels of specific activity of the FeS enzyme aconitase were determined in mitochodrial extracts of the Δ*yfh1* (delta-yfh1) mutant transformed with *T. vaginalis* frataxin (Tvfrataxin), a chimeric construct containing the mitochondrial-targeting sequence of CoxIV (CoxIV-Tvfrataxin), and a wild copy of the gene (YFH1). The activity of the non-FeS enzyme malate dehydrogenase (MDH) was used as a control. Bars indicate standard deviations; $n = 6$.

The Gal-*T. vaginalis* frataxin transformant grew poorly under these conditions, recapitulating the strong growth defect of the Δ*yfh1* mutant. However, there was a partial restoration of growth in the cells with the Gal-CoxIV-*T. vaginalis* frataxin construct. This result indicates that *T. vaginalis* frataxin can partially complement the function of Yfh1. The complementation requires the presence of the N-terminal targeting sequence from CoxIV to enable the translocation of the protein into the mitochondria. Analysis of yeast cellular fractions (data not shown) revealed that *T. vaginalis* frataxin possessing only the hydrogenosomal-targeting sequence did indeed remain in the cytosol and was not translocated into the mitochondria.

Ability of *T. vaginalis* frataxin to restore FeS cluster and heme synthesis. To examine the molecular basis for the partial restoration of the growth of the Δ*yfh1* mutant by *T. vaginalis* frataxin, we investigated the potential of *T. vaginalis* frataxin to restore FeS cluster and heme synthesis. The activity of the mitochondrial FeS protein aconitase was measured in yeast expressing Yfh1 and *T. vaginalis* frataxin (Fig. 6). Comparison of the aconitase activity of yeast containing the Gal-CoxIV-*T. vaginalis* frataxin construct with the aconitase activities of positive (Gal-Yfh1) and negative controls showed that Gal-CoxIV-*T. vaginalis* frataxin was able to restore about 50% of the specific activity conferred by Gal-Yfh1. There was no restoration of aconitase activity by Gal-*T. vaginalis* frataxin alone, which is consistent with the inability of this construct to improve the growth of the Δ*yfh1* mutant. The partial complementation of aconitase activity by CoxIV-*T. vaginalis* frataxin suggests that the trichomonad homologue, when present in the mitochondria, may cooperate with yeast IscU and participate in FeS cluster formation. Malate dehydrogenase, the activity of which is not dependent on FeS cluster formation, was not affected in the Gal-*T. vaginalis* frataxin and Δ*yfh1* mutants (Fig. 5).

Low-temperature spectra of whole cells were recorded to evaluate the levels of heme synthesis. Colonies of the Δ*yfh1* mutant are known to be depigmented as the result of general heme deficiency. In our experiment, the Gal-CoxIV-*T. vaginalis* frataxin strain showed increased levels of cytochrome (*b* and *c*) signals in comparison with the levels in the Δ*yfh1* mutant (Fig. 7). Interestingly, a clear signal from zinc protoporphyrin was observed in the complemented strain. The accumulation of zinc protoporphyrin, which is a feature of the Δ*yfh1* phenotype, reflects inadequate iron or unavailable iron (23). The Gal-CoxIV-*T. vaginalis* frataxin strain partially complemented the deletion, suggesting that CoxIV-*T. vaginalis* frataxin is able to interact at low efficiency in vivo with yeast ferrochelatase.

***T. vaginalis* frataxin and ferrochelatase interact in vitro.** To investigate the interaction of *T. vaginalis* frataxin with its pre-

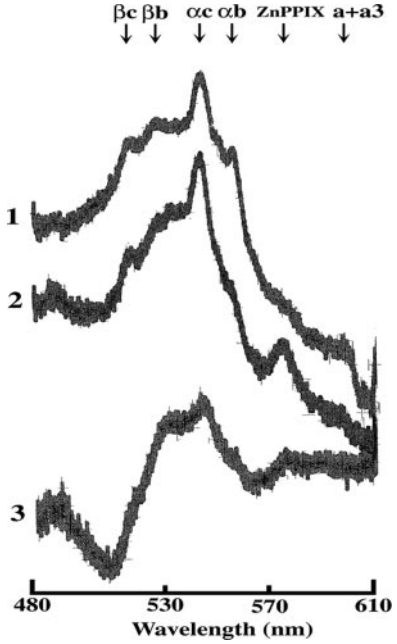

FIG. 7. Cytochrome composition in the complemented yeast strain. Low-temperature spectra of whole cells of the Yfh1 shuffle strain with integrated Gal-*YFH1* (1), Gal-CoxIV-*T. vaginalis* frataxin (2), and vector alone (3). In cells complemented with *T. vaginalis* frataxin, zinc protoporphyrin accumulated, indicating inefficient iron administration of *T. vaginalis* frataxin to ferrochelatase.

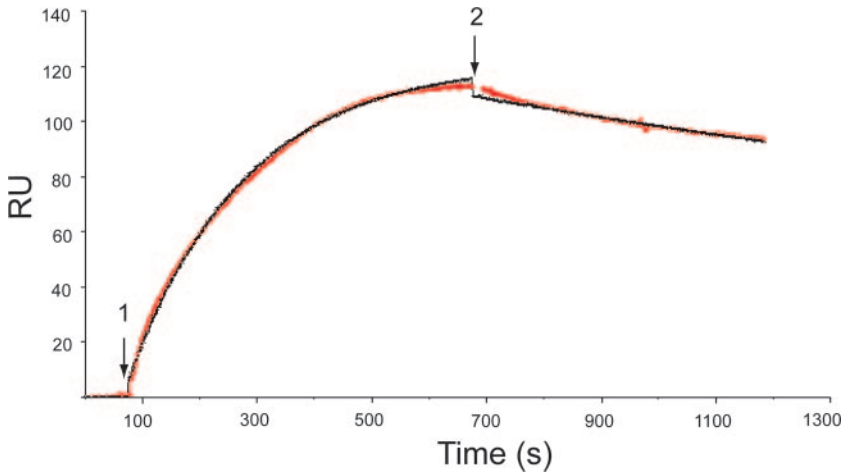

FIG. 8. *T. vaginalis* frataxin and yeast ferrochalatase interact in vitro. Typical sensorgram obtained when measuring the interaction of 1×10^{-7} M purified ferrochelatase in the running buffer injected over 200 RU immobilized *T. vaginalis* frataxin (1). Dissociation of the *T. vaginalis* frataxin-ferrochelatase complex was analyzed after removal of Yfh1p from the mobile phase (2). The solid black line over the curve represents the best fit of the experimental data with a 1:1 Langmuir model of interaction.

dicted interacting partners, we used a real-time biomolecular interaction analyzer, Biacore 2000. A specific interaction between *T. vaginalis* frataxin and ferrochelatase was measured when ferrochelatase was used as the analyte (Fig. 8), while no interaction was found with bovine serum albumin as a negative control. The dissociation constant was estimated as K_D = 7e-9 by fitting to a simple Langmuir model.

DISCUSSION

Homologues of frataxin are present in organisms ranging from eubacteria to mammalian cells but are absent in archaebacteria. They are highly conserved proteins with no homology identified outside the frataxin family. In *S. cerevisiae* and humans, frataxin is believed to have an important role in mitochondrial iron metabolism (15, 23). The current data demonstrate that hydrogenosomes of *T. vaginalis* also possess functional frataxin and suggest that this protein is likely to participate, either directly or indirectly, in the synthesis of FeS clusters within hydrogenosomes.

The frataxin sequence identified in *T. vaginalis* possesses features typical of the protein family as found for the human and yeast homologues. Conserved acidic residues implicated in iron binding are found at the N terminus of *T. vaginalis* frataxin, suggesting that the protein may possess similar properties in mobilizing iron for its interacting partners (2, 18). For Yfh1, it was shown that its iron-binding residues significantly overlap with those involved in ferrochelatase binding, arguing for iron transfer from frataxin to ferrochelatase (18). Indeed, as demonstrated by the Biacore assay, *T. vaginalis* frataxin is able to interact in vitro with yeast ferrochelatase, the enzyme responsible for catalyzing the insertion of iron into the protoporphyrin ring during mitochondrial heme biosynthesis. Consistently, *T. vaginalis* frataxin is able to partially restore defective heme synthesis in a Δ*yfh1* mutant. However, a fraction of protoporphyrin molecules contained zinc instead of iron in CoxIV-*T. vaginalis* frataxin yeast cells, likely reflecting an inefficient delivery of iron by the heterologous frataxin. Hypothetically, this might be due to the specificity of *T. vaginalis* frataxin for different natural partners, since *T. vaginalis* lacks cytochromes and no components of the heme synthesis pathway, including the homologue of ferrochelatase, have been found in the recently completed *T. vaginalis* genome (9).

Besides an involvement in heme synthesis, the yeast frataxin was shown to physically interact with IscU, a central component of FeS cluster assembly (15). IscU serves as a scaffold molecule for building an FeS cluster intermediate in participation with IscS that provides the required sulfur from free cysteine (3, 47). The transient FeS cluster on IscU is then transferred to the target apoprotein. The detection of frataxin in complex with the IscU/IscS pair suggested that frataxin also participates in FeS cluster assembly—possibly as an iron donor (15). FeS cluster synthesis has already been shown to occur in *T. vaginalis* hydrogenosomes via an IscS-mediated mitochondrial-type system (38). Although IscU has not been characterized in *T. vaginalis*, an IscU homologue is present in the *T. vaginalis* genome (9). Moreover, the homologue possesses a putative hydrogenosomal-targeting sequence, which indicates its potential colocalization with IscS and frataxin within the hydrogenosomal compartment. Thus, it is plausible that an IscS/IscU/frataxin complex is formed in *T. vaginalis* hydrogenosomes and participates in FeS cluster synthesis.

The stimulation of frataxin transcription during iron deficiency may indicate a common mode of regulation with IscS, the transcription of which was also shown to be upregulated in iron deficiency (38). This contrasts with the transcription of key hydrogenosomal proteins involved in energy metabolism and the transport of electrons, which are often FeS proteins and whose transcription is dramatically reduced in the absence of iron (42). The reason for frataxin and IscS upregulation might be the increased cellular demand for new FeS cluster synthesis, although more experimental data are necessary to test this hypothesis. Interestingly, in the yeasts *S. cerevisiae* and *C. albicans*, frataxin transcription was shown to be strongly induced by iron (32, 33). This finding is consistent with the proposed role of frataxin as an iron storage molecule. For example, yeast

Yfh1 was shown to self assemble in an iron-dependent manner and to sequester iron in vitro, and it was proposed that by this mechanism, reminiscent of the function of mammalian ferritin, frataxin keeps iron bioavailable and nontoxic (14, 29). Moreover, the overexpression of newly identified mitochondrial ferritin (8) was able to repair the phenotype of a frataxin-deficient strain, supporting a partial redundancy of these two iron-binding proteins. However, the in vivo relevance of iron-dependent polymerization of Yfh1 was put in question by the ability of modified nonpolymerizing Yfh1 to fully restore the phenotype of a Δ*yfh1* mutant (5).

Recent discoveries in FeS cluster assembly in eukaryotes have underlined the essential role of mitochondria in this process (24, 25). Defects in the expression of components involved in FeS cluster synthesis often have dramatic or even lethal consequences for the whole organism. Consequently, it has been suggested that FeS cluster synthesis might be the critical indispensable function of mitochondria and of the mitochondrial homologues, hydrogenosomes and mitosomes, recently identified in some microaerophilic and parasitic unicellular eukaryotes (22, 38, 41). The finding of a frataxin homologue in the hydrogenosomes of *T. vaginalis* prompted us to search for frataxin homologues in the genomes of these unicellular eukaryotes. Interestingly, no frataxin-like sequence was found in the genomes of *Giardia intestinalis* or *Entamoeba histolytica*, both of which have mitosomes (*Giardia*DB, http://gmod.mbl.edu/perl/site/giardia14?page=orfs) (27). In *Giardia*, components of FeS cluster assembly (IscU, IscS, and ferredoxin) are present in its mitosomes, and the corresponding cellular fraction was demonstrated to catalyze the formation of FeS clusters in vitro (41). Thus, the absence of frataxin in *Giardia* was unexpected. For *Entamoeba*, the situation is more complicated because, uniquely among eukaryotes, *Entamoeba* has lost the genes for the ISC system and instead has acquired genes for the bacterium-like NIF system for the biosynthesis of FeS clusters (4, 44). Thus, *Entamoeba* may not need frataxin. By contrast, frataxin homologues are probably present in the mitosomes of other parasitic eukaryotes. Analysis of the genome of the microsporidian *Encephalitozoon* reveals a homologue of frataxin and other components of the ISC machinery, including IscS, IscU, ferredoxin, Erv1, and ATM1 (21). The genome of *Cryptosporidium parvum* also encodes both IscS and IscU homologues that contain functional mitochondrial-targeting signals, indicating that an ISC machinery operates within its mitosome or remnant mitochondrion (22, 36). The same location is predicted in silico for the *C. parvum* frataxin homologue (1).

In mitochondria, a specific set of proteins ensures the biosynthesis of the iron-containing prosthetic groups, heme and FeS clusters. The study of iron metabolism in the amitochondriate eukaryote *T. vaginalis* shows that within hydrogenosomes, an elaborate homologous system functions in FeS cluster synthesis. While mitochondria and hydrogenosomes differ substantially in the complexity of their metabolism, the same fundamental role of these endosymbiotic organelles in cellular iron metabolism supports their common evolutionary origin. As other mitochondrial homologues also appear to harbor a minimal set of components derived from the endosymbiont that are involved in FeS cluster synthesis, it may be hypothesized that this process was, and still is, an important function of this organelle.

ACKNOWLEDGMENTS

This work was supported by the Grant Agency of the Academy of Sciences of the Czech Republic (A501110631) and with grants MSM0021620858 and LC07032 to J.T. and NIH grant DK53953 to A.D. P.D. is a recipient of a Marie Curie outgoing fellowship.

We thank Robert Hirt for access to unpublished *Trichomonas vaginalis* expressed sequence tag data generated under a Wellcome Trust university award (no. 060068).

REFERENCES

1. **Abrahamsen, M. S., T. J. Templeton, S. Enomoto, J. E. Abrahante, G. Zhu, C. A. Lancto, M. Deng, C. Liu, G. Widmer, S. Tzipori, G. A. Buck, P. Xu, A. T. Bankier, P. H. Dear, B. A. Konfortov, H. F. Spriggs, L. Iyer, V. Anantharaman, L. Aravind, and V. Kapur.** 2004. Complete genome sequence of the apicomplexan, Cryptosporidium parvum. Science **304:**441–445.
2. **Adinolfi, S., M. Trifuoggi, A. S. Politou, S. Martin, and A. Pastore.** 2002. A structural approach to understanding the iron-binding properties of phylogenetically different frataxins. Hum. Mol. Genet. **11:**1865–1877.
3. **Agar, J. N., C. Krebs, J. Frazzon, B. H. Huynh, D. R. Dean, and M. K. Johnson.** 2000. IscU as a scaffold for iron-sulfur cluster biosynthesis: sequential assembly of [2Fe-2S] and [4Fe-4S] clusters in IscU. Biochemistry **39:** 7856–7862.
4. **Ali, V., Y. Shigeta, U. Tokumoto, Y. Takahashi, and T. Nozaki.** 2004. An intestinal parasitic protist, Entamoeba histolytica, possesses a non-redundant nitrogen fixation-like system for iron-sulfur cluster assembly under anaerobic conditions. J. Biol. Chem. **279:**16863–16874.
5. **Aloria, K., B. Schilke, A. Andrew, and E. A. Craig.** 2004. Iron-induced oligomerization of yeast frataxin homologue Yfh1 is dispensable in vivo. EMBO Rep. **5:**1096–1101.
6. **Babcock, M., D. de Silva, R. Oaks, S. Davis-Kaplan, S. Jiralerspong, L. Montermini, M. Pandolfo, and J. Kaplan.** 1997. Regulation of mitochondrial iron accumulation by Yfh1p, a putative homolog of frataxin. Science **276:** 1709–1712.
7. **Camadro, J. M., and P. Labbe.** 1988. Purification and properties of ferrochelatase from the yeast *Saccharomyces cerevisiae*. Evidence for a precursor form of the protein. J. Biol. Chem. **263:**11675–11682.
8. **Campanella, A., G. Isaya, H. A. O'Neill, P. Santambrogio, A. Cozzi, P. Arosio, and S. Levi.** 2004. The expression of human mitochondrial ferritin rescues respiratory function in frataxin-deficient yeast. Hum. Mol. Genet. **13:**2279–2288.
9. **Carlton, J. M., R. P. Hirt, J. C. Silva, A. L. Delcher, M. Schatz, Q. Zhao, J. R. Wortman, S. L. Bidwell, U. C. Alsmark, S. Besteiro, T. Sicheritz-Ponten, C. J. Noel, J. B. Dacks, P. G. Foster, C. Simillion, Y. Van de Peer, D. Miranda-Saavedra, G. J. Barton, G. D. Westrop, S. Müller, D. Dessi, P. L. Fiori, Q. Ren, I. Paulsen, H. Zhang, F. D. Bastida-Corcuera, A. Simoes-Barbosa, M. T. Brown, R. D. Hayes, M. Mukherjee, C. Y. Okumura, R. Schneider, A. J. Smith, S. Vanacova, M. Villalvazo, B. J. Haas, M. Pertea, T. V. Feldblyum, T. R. Utterback, C. L. Shu, K. Osoegawa, P. J. de Jong, I. Hrdy, L. Horvathova, Z. Zubacova, P. Dolezal, S. B. Malik, J. M. Logsdon, Jr., K. Henze, A. Gupta, C. C. Wang, R. L. Dunne, J. A. Upcroft, P. Upcroft, O. White, S. L. Salzberg, P. Tang, C. H. Chiu, Y. S. Lee, T. M. Embley, G. H. Coombs, J. C. Mottram, J. Tachezy, C. M. Fraser-Liggett, and P. J. Johnson.** 2007. Draft genome sequence of the sexually transmitted pathogen *Trichomonas vaginalis*. Science **315:**207–212.
10. **Cho, S. J., M. G. Lee, J. K. Yang, J. Y. Lee, H. K. Song, and S. W. Suh.** 2000. Crystal structure of *Escherichia coli* CyaY protein reveals a previously unidentified fold for the evolutionarily conserved frataxin family. Proc. Natl. Acad. Sci. USA **97:**8932–8937.
11. **Condo, I., N. Ventura, F. Malisan, B. Tomassini, and R. Testi.** 2006. A pool of extramitochondrial frataxin that promotes cell survival. J. Biol. Chem. **281:**16750–16756.
12. **Dhe-Paganon, S., R. Shigeta, Y. I. Chi, M. Ristow, and S. E. Shoelson.** 2000. Crystal structure of human frataxin. J. Biol. Chem. **275:**30753–30756.
13. **Durr, A.** 2002. Friedreich's ataxia: treatment within reach. Lancet Neurol. **1:**370–374.
14. **Gakh, O., J. Adamec, A. M. Gacy, R. D. Twesten, W. G. Owen, and G. Isaya.** 2002. Physical evidence that yeast frataxin is an iron storage protein. Biochemistry **41:**6798–6804.
15. **Gerber, J., K. Neumann, C. Prohl, U. Mühlenhoff, and R. Lill.** 2004. The yeast scaffold proteins Isu1p and Isu2p are required inside mitochondria for maturation of cytosolic Fe/S proteins. Mol. Cell. Biol. **24:**4848–4857.
16. **Gora, M., E. Grzybowska, J. Rytka, and R. Labbe-Bois.** 1996. Probing the active-site residues in *Saccharomyces cerevisiae* ferrochelatase by directed mutagenesis. In vivo and in vitro analyses. J. Biol. Chem. **271:**11810–11816.
17. **Gordon, D. M., M. Kogan, S. A. Knight, A. Dancis, and D. Pain.** 2001. Distinct roles for two N-terminal cleaved domains in mitochondrial import of the yeast frataxin homolog, Yfh1p. Hum. Mol. Genet. **10:**259–269.
18. **He, Y., S. L. Alam, S. V. Proteasa, Y. Zhang, E. Lesuisse, A. Dancis, and T. L. Stemmler.** 2004. Yeast frataxin solution structure, iron binding, and ferrochelatase interaction. Biochemistry **43:**16254–16262.

19. **Hrdy, I., R. P. Hirt, P. Dolezal, L. Bardonova, P. G. Foster, J. Tachezy, and T. M. Embley.** 2004. Trichomonas hydrogenosomes contain the NADH dehydrogenase module of mitochondrial complex I. Nature **432:**618–622.
20. **Karthikeyan, G., J. H. Santos, M. A. Graziewicz, W. C. Copeland, G. Isaya, B. Van Houten, and M. A. Resnick.** 2003. Reduction in frataxin causes progressive accumulation of mitochondrial damage. Hum. Mol. Genet. **12:** 3331–3342.
21. **Katinka, M. D., S. Duprat, E. Cornillot, G. Metenier, F. Thomarat, G. Prensier, V. Barbe, E. Peyretaillade, P. Brottier, P. Wincker, F. Delbac, A. H. El Alaoui, P. Peyret, W. Saurin, M. Gouy, J. Weissenbach, and C. P. Vivares.** 2001. Genome sequence and gene compaction of the eukaryote parasite *Encephalitozoon cuniculi*. Nature **414:**450–453.
22. **LaGier, M. J., J. Tachezy, F. Stejskal, K. Kutisova, and J. S. Keithly.** 2003. Mitochondrial-type iron-sulfur cluster biosynthesis genes (IscS and IscU) in the apicomplexan *Cryptosporidium parvum*. Microbiology **149:**3519–3530.
23. **Lesuisse, E., R. Santos, B. F. Matzanke, S. A. Knight, J. M. Camadro, and A. Dancis.** 2003. Iron use for haeme synthesis is under control of the yeast frataxin homologue (Yfh1). Hum. Mol. Genet. **12:**879–889.
24. **Li, J., M. Kogan, S. A. Knight, D. Pain, and A. Dancis.** 1999. Yeast mitochondrial protein, Nfs1p, coordinately regulates iron-sulfur cluster proteins, cellular iron uptake, and iron distribution. J. Biol. Chem. **274:**33025–33034.
25. **Lill, R., and G. Kispal.** 2000. Maturation of cellular Fe-S proteins: an essential function of mitochondria. Trends Biochem. Sci. **25:**352–356.
26. **Liston, D. R., and P. J. Johnson.** 1999. Analysis of a ubiquitous promoter element in a primitive eukaryote: early evolution of the initiator element. Mol. Cell. Biol. **19:**2380–2388.
27. **Loftus, B., I. Anderson, R. Davies, U. C. Alsmark, J. Samuelson, P. Amedeo, P. Roncaglia, M. Berriman, R. P. Hirt, B. J. Mann, T. Nozaki, B. Suh, M. Pop, M. Duchene, J. Ackers, E. Tannich, M. Leippe, M. Hofer, I. Bruchhaus, U. Willhoeft, A. Bhattacharya, T. Chillingworth, C. Churcher, Z. Hance, B. Harris, D. Harris, K. Jagels, S. Moule, K. Mungall, D. Ormond, R. Squares, S. Whitehead, M. A. Quail, E. Rabbinowitsch, H. Norbertczak, C. Price, Z. Wang, N. Guillen, C. Gilchrist, S. E. Stroup, S. Bhattacharya, A. Lohia, P. G. Foster, T. Sicheritz-Ponten, C. Weber, U. Singh, C. Mukherjee, N. M. El-Sayed, W. A. Petri, Jr., C. G. Clark, T. M. Embley, B. Barrell, C. M. Fraser, and N. Hall.** 2005. The genome of the protist parasite *Entamoeba histolytica*. Nature **433:**865–868.
28. **McAlister-Henn, L., and L. M. Thompson.** 1987. Isolation and expression of the gene encoding yeast mitochondrial malate dehydrogenase. J. Bacteriol. **169:**5157–5166.
29. **O'Neill, H. A., O. Gakh, S. Park, J. Cui, S. M. Mooney, M. Sampson, G. C. Ferreira, and G. Isaya.** 2005. Assembly of human frataxin is a mechanism for detoxifying redox-active iron. Biochemistry **44:**537–545.
30. **Raguzzi, F., E. Lesuisse, and R. R. Crichton.** 1988. Iron storage in *Saccharomyces cerevisiae*. FEBS Lett. **231:**253–258.
31. **Rouault, T. A.** 2006. The role of iron regulatory proteins in mammalian iron homeostasis and disease. Nat. Chem. Biol. **2:**406–414.
32. **Santos, R., N. Buisson, S. A. Knight, A. Dancis, J. M. Camadro, and E. Lesuisse.** 2004. *Candida albicans* lacking the frataxin homologue: a relevant yeast model for studying the role of frataxin. Mol. Microbiol. **54:**507–519.
33. **Santos, R., A. Dancis, D. Eide, J. M. Camadro, and E. Lesuisse.** 2003. Zinc suppresses the iron-accumulation phenotype of *Saccharomyces cerevisiae* lacking the yeast frataxin homologue (Yfh1). Biochem. J. **375:**247–254.
34. **Schilke, B., C. Voisine, H. Beinert, and E. Craig.** 1999. Evidence for a conserved system for iron metabolism in the mitochondria of *Saccharomyces cerevisiae*. Proc. Natl. Acad. Sci. USA **96:**10206–10211.
35. **Schwede, T., J. Kopp, N. Guex, and M. C. Peitsch.** 2003. SWISS-MODEL: an automated protein homology-modeling server. Nucleic Acids Res. **31:**3381–3385.
36. **Slapeta, J., and J. S. Keithly.** 2004. *Cryptosporidium parvum* mitochondrial-type HSP70 targets homologous and heterologous mitochondria. Eukaryot. Cell **3:**483–494.
37. **Smid, O., E. Horakova, V. Vilimova, I. Hrdy, R. Cammack, A. Horvath, J. Lukes, and J. Tachezy.** 2006. Knock-downs of iron-sulfur cluster assembly proteins IscS and IscU down-regulate the active mitochondrion of procyclic *Trypanosoma brucei*. J. Biol. Chem. **281:**28679–28686.
38. **Sutak, R., P. Dolezal, H. L. Fiumera, I. Hrdy, A. Dancis, M. Delgadillo-Correa, P. J. Johnson, M. Müller, and J. Tachezy.** 2004. Mitochondrial-type assembly of FeS centers in the hydrogenosomes of the amitochondriate eukaryote *Trichomonas vaginalis*. Proc. Natl. Acad. Sci. USA **101:**10368–10373.
39. **Tachezy, J., L. B. Sanchez, and M. Müller.** 2001. Mitochondrial type iron-sulfur cluster assembly in the amitochondriate eukaryotes *Trichomonas vaginalis* and *Giardia intestinalis*, as indicated by the phylogeny of IscS. Mol. Biol. Evol. **18:**1919–1928.
40. **Thompson, J. D., T. J. Gibson, F. Plewniak, F. Jeanmougin, and D. G. Higgins.** 1997. The CLUSTAL_X Windows interface: flexible strategies for multiple sequence alignment aided by quality analysis tools. Nucleic Acids Res. **25:**4876–4882.
41. **Tovar, J., G. Leon-Avila, L. B. Sanchez, R. Sutak, J. Tachezy, M. van der Giezen, M. Hernandez, M. Müller, and J. M. Lucocq.** 2003. Mitochondrial remnant organelles of Giardia function in iron-sulphur protein maturation. Nature **426:**172–178.
42. **Vanacova, S., D. Rasoloson, J. Razga, I. Hrdy, J. Kulda, and J. Tachezy.** 2001. Iron-induced changes in pyruvate metabolism of *Tritrichomonas foetus* and involvement of iron in expression of hydrogenosomal proteins. Microbiology **147:**53–62.
43. **Vanacova, S., J. Tachezy, E. Ullu, and C. Tschudi.** 2001. Unusual diversity in alpha-amanitin sensitivity of RNA polymerases in trichomonads. Mol. Biochem. Parasitol. **115:**239–247.
44. **van der Giezen, M., S. Cox, and J. Tovar.** 2004. The iron-sulfur cluster assembly genes iscS and iscU of *Entamoeba histolytica* were acquired by horizontal gene transfer. BMC Evol. Biol. **4:**7.
45. **Wilson, R. B., and D. M. Roof.** 1997. Respiratory deficiency due to loss of mitochondrial DNA in yeast lacking the frataxin homologue. Nat. Genet. **16:**352–357.
46. **Yoon, T., and J. A. Cowan.** 2003. Iron-sulfur cluster biosynthesis. Characterization of frataxin as an iron donor for assembly of [2Fe-2S] clusters in ISU-type proteins. J. Am. Chem. Soc. **125:**6078–6084.
47. **Yuvaniyama, P., J. N. Agar, V. L. Cash, M. K. Johnson, and D. R. Dean.** 2000. NifS-directed assembly of a transient [2Fe-2S] cluster within the NifU protein. Proc. Natl. Acad. Sci. USA **97:**599–604.
48. **Zhang, Y., E. R. Lyver, S. A. Knight, E. Lesuisse, and A. Dancis.** 2005. Frataxin and mitochondrial carrier proteins, Mrs3p and Mrs4p, cooperate in providing iron for heme synthesis. J. Biol. Chem. **280:**19794–19807.